Blind Interference Alignment in multi-cell mmWave access and fronthaul

Vaia Kalokidou, Angela Doufexi, Mark Beach
Communication Systems and Networks Group
University of Bristol
Bristol, UK
{vaia.kalokidou,a.doufexi,m.a.beach@bristol.ac.uk}

***Abstract*—Enhanced network capacity and reduced overhead will be some of the future communication networks requirements. In the absence of Channel State Information (CSI) at the transmitter, Blind Interference Alignment (Blind IA) has shown that optimal Degrees of Freedom (DoF) can be achieved, minimizing network's overhead. Limited spectrum is a basic issue that millimeter-Wave (mmWave) frequencies can resolve in 5G systems. Our contribution is an interference management scheme, based on Blind IA that can be employed in multi-cell, slow-fading, mmWave networks. Blind IA manages inter- and intra-cell interference by antenna selection and appropriate message scheduling. We show that our proposed scheme achieves considerably higher sum rate than TDMA, and overall outperforms TDMA in terms of Degrees of Freedom (DoF) in most cases. Also, Blind IA provides better Bit Error Rate (BER) performance and fairness, in terms of scheduling, to the network users.**

Keywords—blind interference alignment, mmWave, beamforming, interference management

I. Introduction

Cellular and wireless networks have been recently challenged by the increasing number of mobile Internet services and the constant growth of mobile data traffic. Fifth generation (5G) networks should provide reduced latency, improved energy efficiency, and high user data rates in dense network environments. Due to the current limited frequency spectrum, mmWave technology, offering a wide range of frequencies, can provide the required bandwidth to support high data rates. mmWave frequencies are considered both for access and fronthaul (FH) (transport links), especially for areas where optical fiber is difficult to install. However, mmWave channels suffer from high propagation loss, and thus require highly directional beamforming [1].

Digital precoding, due to its complexity and increased cost, is not considered as an implementation solution in mmWave, although it provides higher Degrees of Freedom (DoF) [1]. A popular solution in mmWave systems is analogue beamforming, which provides high beamforming gains and is based on simple designs but reduces the flexibility of the system. It is usually implemented through RF phase shifters, which connect to one RF chain and control the phase of the signal at each antenna [2, 3]. In addition, adaptive analogue beamforming, proposed in [4], based on transmitter and receiver jointly selecting the optimal beamforming vector, can maximise received signal power.

A combination of digital and analogue beamforming, known as hybrid beamforming constitutes another implementation solution in mmWave. Antennas can be connected either fully, increasing flexibility, or partially, reducing the complexity, to each RF chain.

Another challenge will be the employment of novel interference management strategies that will manage interference, without increasing the system's overhead, and provide high data rates and reliable transmissions. Interference Alignment (IA) was introduced by Maddah-Ali et al. in [5], and Jafar et al. in [6] for the MIMO X channels, and by Cadambe et al. in [7] for the K-user interference channel, where $K/2$ DoF can be achieved. However, the main drawbacks of IA were the requirement of perfect and global CSI and computational complexity.

Further work on IA led to the scheme of Blind IA, presented by Wang, et al. in [8] and Jafar in [9], for certain network scenarios, which can achieve full DoF in the absence of CSI at the transmitters (CSIT), thus reducing the system overhead. Moreover, Blind IA was introduced, by Jafar in [10], for cellular and heterogeneous networks, by "seeing" frequency reuse as a simple form of IA. Blind IA in heterogeneous networks was generalized in [11], introducing Kronecker (Tensor) Product representation and a variation of model parameters to optimize the sum rate performance.

In the context of mmWave, initial research has shown that IA is considered as a possible solution in 5G systems. In [12], authors investigate the feasibility of IA in mmWave systems, by identifying the conditions under which mmWave networks operate in the interference-limited regime. Moreover, authors in [13] propose an IA scheme for 3-cell mmWave mobile networks, investigating the sum-rate capacity.

In [11], we introduced a Blind IA scheme, without looking into a particular frequency band, possible applications in 4G/5G networks, and without examining full inter-cell interference. In this paper, based on [11], we introduce a Blind IA scheme in mmWave multi-cell networks, i.e. considering mmWave channels, based on partially-connected antennas beamforming, where the codebook is constructed to fully mitigate inter- and intra-cell interference. From now on, to consider the cases of both access and FH, reference to 'users' can also refer to mmWave Access Points (APs). In that case, the reference to 'main cell' and 'neighbouring cell' is not valid, as every AP will correspond to a cell. We consider a K-user main cell and K neighbouring cells, serving one user each. Our contribution is the consideration of inter- and intra-cell interference in all cells, of the position of every user, and the employment of Blind IA in mmWave systems. Moreover, we show the DoF advantage of Blind IA over Time Division Multiple Access (TDMA). The Blind IA algorithm is described by using Kronecker product representation and optimisation of the sum rate.

II. System Model

Consider the mmWave Broadcast Channel (BC) of a multi-cell network, as shown in Fig. 1, with 1 main cell and K neighbouring cells. At the $N \times N$ BC of the *main cell*, there is one transmitter T_{x_A} (equipped with a large uniform linear array (ULA)) with N antennas and K RF chains, and K users equipped with N antennas and RF chains each. Transmitter T_{x_A} has N messages to send to every user, and when it transmits to user a_k, where $k \in \{1,2,\dots,K\}$, it causes interference to the other $K-1$ users in the main cell and the neighbouring cell user f_k. A neighbouring cell is considered to interfere with every user in the main cell. At the $M_r \times N$ BC of each *neighbouring cell*, there is one transmitter $T_{x_{Fk}}$ (equipped with a large ULA) with N antennas and one RF chain, and one user f_k can be equipped with $M_r = N-1$ or $M_r = N$ antennas. When transmitter $T_{x_{Fk}}$ transmits $\mathcal{M} = (K-1)(M_r-1)+1$ messages to user f_k, it causes interference to the main cell user a_k. We consider that all channels remain constant over $\mathrm{T} = \mathrm{K}+1$ time slots (i.e. supersymbol) and the position of users in the cells, as summarised in Table I. Notations (number of antennas/users/etc.) are defined in such a way to provide the maximum possible DoF in the network (based on an analysis not given in this paper due to space limitations).

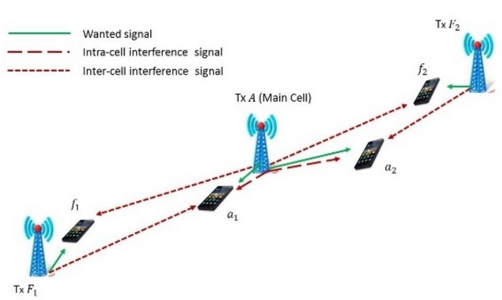

Fig. 1. Example model of Multi-cell mmWave network

We consider the following example model: In the main cell, there are $K=2$ users, $N=2$ messages intended for every user and transmit and receive antennas. Additionally, there are $K=2$ neighbouring cells, with $N=M_r=2$ transmit and receive antennas each, and $\mathcal{M}=2$ messages are intended for every user in the neighbouring cells. The channels remain constant for $T=3$ time slots.

In the main cell, the $NT \times 1$ signal at receiver a_k, for the supersymbol considering slow fading, is given by:

$$\boldsymbol{y}_{a_k} = \boldsymbol{H}_{a_k}\boldsymbol{x}_A + \boldsymbol{H}_{f_k a_k}\boldsymbol{x}_{f_k} + \boldsymbol{z}_{a_k}, \tag{1}$$

where $\boldsymbol{H}_{a_k} \in \mathbb{C}^{(TN\times TN)}$ is the channel transfer matrix from T_{x_A} to receiver a_k and is given by $\boldsymbol{H}_{a_k} = \sqrt{\gamma_{a_k}}(\boldsymbol{I}_T \otimes \boldsymbol{h}_{a_k})$ (here and throughout $\boldsymbol{H}_k = \sqrt{\gamma_k}(\boldsymbol{I}_T \otimes \boldsymbol{h}_k)$ with $\boldsymbol{h}_k$ denoting the channel coefficients from T_{x_k} to k for one time slot, $\gamma_k = 1/d_k^n$ the path loss of user k with n denoting the path loss exponent considered for a mmWave urban environment, $n=\{2,3\}$, and $\otimes$ the Kronecker product). $\boldsymbol{H}_{f_k a_k} \in \mathbb{C}^{(TN\times TM_r)}$ is the interference channel transfer matrix from $T_{x_{Fk}}$ to receiver a_k. Due to the users' different locations, channel coefficients are statistically independent, and follow an i.i.d. Gaussian distribution $\mathcal{CN}(0,1)$. Finally, $\boldsymbol{z}_{a_k} \backsim \mathcal{CN}(0, \sigma_n^2 \boldsymbol{I}_T)$ denotes the independent Additive White Gaussian Noise (AWGN) at the input of receiver a_k.

Table I. Distance Metrics for example model

Description	Value
mmWave cell radius	200m
Reuse Distance main-neighbouring cell	100m
Distance of a_1 from T_{x_A}	20m
Distance of a_2 from T_{x_A}	70m
Distance of f_1 from $T_{x_{F_1}}$	20m
Distance of f_2 from $T_{x_{F_2}}$	10m

The channel, based on the model proposed by R.W. Heath (eq. 4 in [14]), is expressed as:

$$\boldsymbol{H} = \sqrt{\frac{N_{BS}N_{MS}}{\rho}} \sum_{l=1}^{L} \alpha_l \ \boldsymbol{a}_{MS}(\theta_l) a_{BS}^H(\phi_l), \tag{2}$$

where N_{BS}, N_{MS} denote the number of antennas at the base station (BS) and the mobile station (MS) respectively, ρ is the average path-loss between the BS and the MS, α_l expresses the complex gain of the l^{th} path, and $\boldsymbol{a}_{BS}(\phi_l), \boldsymbol{a}_{MS}(\theta_l)$ denote the array response vectors at the BS and MS respectively. For all the simulations in this paper, we have considered number of paths as $l=4$.

The total transmit power, as initially presented in [11], is given by the power constraint:

$$P_{main\ cell} = \mathbb{E}[\mathrm{tr}(\boldsymbol{X}_A \boldsymbol{X}_A^T)] = KN\alpha^2 \tag{3}$$

Then, the $NT \times 1$ transmitted vector $\boldsymbol{x}_A$ is given by:

$$\boldsymbol{x}_A = \sum_{k=1}^{K} \boldsymbol{V}_{a_k} \boldsymbol{u}_{a_k}, \tag{4}$$

where $\boldsymbol{u}_{a_k}$ is the $N \times 1$ data stream vector of each user a_k, and $\boldsymbol{V}_{a_k}$ is the $NT \times N$ beamforming matrix of user a_k. As mentioned in [11], the choice of the beamforming matrices carrying messages to users in the main cell is not unique and should lie in a space that is orthogonal to the channels of the other $K-1$ users in the main cell. The beamforming matrix, for user a_k, is given by:

$$\boldsymbol{V}_{a_k} = \frac{\alpha}{\sqrt{N}}(\boldsymbol{v}_{a_k} \otimes \boldsymbol{I}_N), \tag{5}$$

where $\alpha \in \mathbb{R}$ is a constant determined by power considerations (see eq. (3)) and $T \times 1$ $\boldsymbol{v}_{a_k}$ should be a unit vector with entries equal to c, $\sqrt{1-c^2}$ (for $c \in \mathbb{R}$ and $c \neq 0, \pm 1$) or 0, with a different combination for every a_k. For every main cell user, there will be one time slot in which only they will be receiving messages and another slot (time slot 1 in Fig. 2) over which T_{x_A} will transmit to all users. Parameter c is used to optimise the rate of the network as explained in Section II-B.

Example 1. The beamforming matrices, as shown in Fig. 2, are given by:

$$\boldsymbol{V}_{a_1} = \frac{a}{\sqrt{N}}\left(\boldsymbol{v}_{a_1} \otimes \boldsymbol{I}_2\right) = \frac{a}{\sqrt{2}}\left([c \quad \sqrt{1-c^2} \quad 0]^T \otimes \boldsymbol{I}_2\right)$$
$$\boldsymbol{V}_{a_2} = \frac{a}{\sqrt{N}}\left(\boldsymbol{v}_{a_2} \otimes \boldsymbol{I}_2\right) = \frac{a}{\sqrt{2}}\left([c \quad 0 \quad \sqrt{1-c^2}]^T \otimes \boldsymbol{I}_2\right).$$

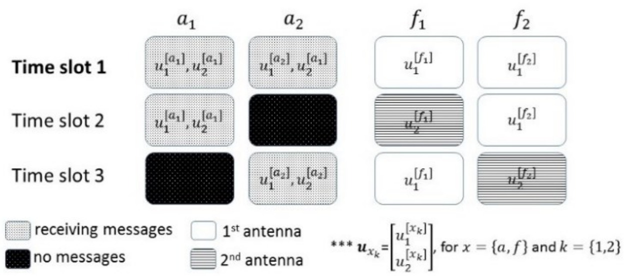

Fig. 2. Beamforming in the main and neighbouring cells.

At each neighbouring cell, the $M_r \times 1$ signal at receiver f_k, for the supersymbol, is given by:

$$\boldsymbol{y}_{f_k} = \boldsymbol{H}_{f_k}\boldsymbol{x}_{f_k} + \boldsymbol{H}_{Af_k}\boldsymbol{x}_A + \boldsymbol{z}_{f_k.} \tag{6}$$

The total transmit power is given by the power constraint:

$$P_{ncell\,F_k} = \mathcal{M}\frac{b}{M_r}, \tag{7}$$

and the $M_r \times 1$ vector, transmitted by $T_{x_{Fk}}$ is given by:

$$\boldsymbol{x}_{f_k} = \boldsymbol{V}_{f_k}\boldsymbol{u}_{f_k}, \tag{8}$$

where $\boldsymbol{u}_{f_k}$ is the $\mathcal{M} \times 1$ data stream vector of each user $f_k$and $\boldsymbol{V}_{f_k}$ the $NT \times \mathcal{M}$ beamforming matrix given by:

$$\boldsymbol{V}_{f_k} = \frac{b}{\sqrt{M_r}}\left(\sum_{i=1}^{T}\xi_{i\,f_k}^T \otimes \boldsymbol{r}_i\boldsymbol{q}_i\right), \tag{9}$$

where $b \in \mathbb{R}$ is a constant determined by power considerations (see eq. (6)), and$\boldsymbol{v}_{1\,f_k} = \sum_{i=1}^{T-1}\xi_{i\,f_k}$ and $\boldsymbol{v}_{2\,f_k} = \xi_{i\,f_k}$ are $1 \times T$ vectors. For $i = 1, \dots, T-1$, $\xi_{i\,f_k}$ has one entry equal to d (for $d\epsilon\mathbb{R}$ and $d \neq 0, \pm\sqrt{\frac{1}{(T-1)(M_r-1)}}$), and $T-1$ entries equal to 0, such that $\boldsymbol{v}_{1\,f_k} = \sum_{i=1}^{T-1}\xi_{i\,f_k}$ has $T-1$ entries equal to d and one entry equal to 0. Vector $\boldsymbol{v}_{2\,f_k}$ has only its $t_1{}^{th}$ entry (t_1 denoting the time slot that a_k receives no interference) equal to $\sqrt{1-(T-1)(M_r-1)d^2}$ and all the rest equal to 0, such that $\sum_{j=1}^{2}\boldsymbol{v}_{j\,f_k}$ has no zero elements for every k. Parameter d is used to optimise the rate in the system as explained in Section II-B.

• If $M_r = N$, for $i = 1, \dots, T-1$, we set $\boldsymbol{r}_i$ equal to the first $N-1$ columns of $\boldsymbol{I}_N$ with $\boldsymbol{e}_1$ equal to the sum of the columns of $\boldsymbol{r}_i$, and $\boldsymbol{e}_2 = \boldsymbol{r}_T$ equal to the last column of $\boldsymbol{I}_N$ (Fig. 3 left).

• If $M_r = N-1$, for $i = 1, \dots, T-1$, we set $\boldsymbol{r}_i$ equal to the sum of the first M_r columns of $\boldsymbol{I}_N$ with $\boldsymbol{e}_1 = \boldsymbol{r}_i$ for any i, and $\boldsymbol{e}_2 = \boldsymbol{r}_T$ equal to the last column of $\boldsymbol{I}_N$ (Fig. 3 right).

Furthermore, for $i = 1, \dots, -1$ and $i \neq t_2$ (t_2 denoting the time slot that T_{x_A} transmits to all users in the main cell), $\boldsymbol{q}_i$ is equal to the submatrix of $\boldsymbol{I}_{\mathcal{M}}$ consisting of rows $(M_r(i-1)+1, M_r i)$, and $\boldsymbol{q}_T$ is equal to the submatrix of $\boldsymbol{I}_{\mathcal{M}}$ consisting of row $\mathcal{M}$, and $\boldsymbol{q}_{t_2}$ is equal to any one of $\boldsymbol{q}_i$ for $i = 1, \dots, T-1$ and $i \neq t_2$. The tth component of $\xi_{i\,f_k}$ being 1 means that in the kth neighbouring cell, the antennas determined by $\boldsymbol{r}_i$are in use at time t, and the messages determined by $\boldsymbol{q}_i$ are transmitted.

Example 2. The beamforming matrix for user f_1, as depicted in Fig. 2, are given by:

$$\boldsymbol{V}_{f_1} = \frac{b}{\sqrt{2}}\left(\sum_{i=1}^{3}\xi_{i\,f_1}^T \otimes \boldsymbol{r}_i\boldsymbol{q}_i\right),$$

with
$$\sum_{i=1}^{2}\xi_{i\,f_1} = \boldsymbol{v}_{1\,f_k} = [d \quad 0 \quad d],$$
$$\xi_{3\,f_k} = \boldsymbol{v}_{2\,f_k} = \left[0 \quad \sqrt{1-2d^2} \quad 0\right]$$

For $i = 1,2$:

$$\boldsymbol{r}_i = \boldsymbol{e}_1 = [1 \quad 0]^T, \boldsymbol{r}_3 = \boldsymbol{e}_2 = [0 \quad 1]^T,$$

and $\boldsymbol{q}_i$ the ith unit basis vector where:

$$\boldsymbol{q}_1 = \boldsymbol{q}_2 = [1 \quad 0], \boldsymbol{q}_3 = [0 \quad 1].$$

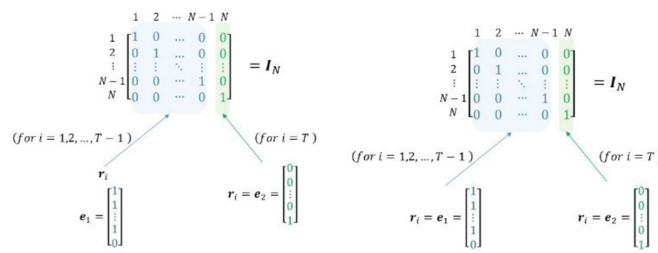

Fig. 3. Design of $\boldsymbol{e}_i, \boldsymbol{r}_i$: (left) $M_r = N$, (right) $M_r = N-1$

A. Interference Management

In all mmWave cells, in order to remove inter- and intra-cell interference, the received signal should be projected to a subspace orthogonal to the subspace that interference lies in.

Definition 1. In the main cell, the rows of the $N \times NT$ projection matrix $\boldsymbol{P}_{a_k} = \sum_{s=1}^{2}\left(\boldsymbol{w}_{s\,a_k} \otimes \left(\boldsymbol{D}_{s\,a_k}\widetilde{\boldsymbol{h}}_{f_k a_k}\right)\right)$, form an orthonormal basis of this subspace, where
1. for all s, the $1 \times T$ $\boldsymbol{w}_{s\,a_k}$ is a unit vector orthogonal to $\boldsymbol{v}_{a_k}$ for $i \neq k$,
2. $\boldsymbol{w}_{s\,a_k}$ has coefficients equal to zero on the non-zero values of $\xi_{i\,f_k}^T$ for $i = 1,2,\dots,T-1$, $s = 2$, and $\xi_{i\,f_k}^T$ for $i = T$, $s = 1$,
3. $\boldsymbol{D}_{1a_k} = diag(\boldsymbol{e}_2)$ and $\boldsymbol{D}_{2a_k} = diag(\boldsymbol{e}_1)$,
4. $\widetilde{\boldsymbol{h}}_{f_k a_k}$ is an $N \times M_r$ matrix, whose rows are unit vectors, with the Nth row orthogonal to all the columns of $\boldsymbol{h}_{f_k a_k}\boldsymbol{e}_1$, and the remaining $N-1$ rows orthogonal to the columns of $\boldsymbol{h}_{f_k a_k}\boldsymbol{e}_2$.

Theorem 1. *Multiplying the received signal by* $\boldsymbol{P}_{a_k}$

$$\widetilde{\boldsymbol{y}}_{a_k} = \boldsymbol{P}_{a_k}\boldsymbol{y}_{a_k} = \boldsymbol{\mathcal{H}}_{a_k}\boldsymbol{u}_{a_k} + \widetilde{\boldsymbol{z}_{a_k}}, \tag{10}$$

where

$$\boldsymbol{\mathcal{H}}_{a_k} = \frac{a}{\sqrt{N}}\boldsymbol{\mathcal{D}}_{a_k}\boldsymbol{\mathcal{K}}_{a_k}, \tag{11}$$

$$\boldsymbol{\mathcal{D}}_{a_k} = \sum_{s=1}^{2}\left(\boldsymbol{w}_{s\,a_k}\boldsymbol{v}_{\,a_k}\boldsymbol{D}_{s\,a_k}\right) = \mathrm{diag}\left(\boldsymbol{w}_{s\,a_k}\boldsymbol{v}_{\,a_k}\right), \quad (12)$$

$$\boldsymbol{\mathcal{K}}_{a_k} = \sqrt{\gamma_{a_k}}\widetilde{\boldsymbol{h}}_{f_k a_k}\boldsymbol{h}_{a_k}, \quad (13)$$

and $\widetilde{\boldsymbol{z}_{a_k.}} = \boldsymbol{P}_{a_k}\boldsymbol{z}_{a_k.}$ *remains white noise with the same variance, since* $\boldsymbol{w}_{s\,a_k}$ *is a unit vector.*

Proof. We show that $\boldsymbol{P}_{a_k}$ removes intra- and inter-cell interference at the kth receiver. Substituting eqs. (1) and (4) in eq. (10), we consider coefficients of $\boldsymbol{u}_{\,a_k}, \boldsymbol{u}_{\,f_k}$ separately. For $i \neq k$, using $(A \otimes B)(C \otimes D) = AC \otimes BD$, coefficient of $\boldsymbol{u}_{\,a_i}$ becomes:

$$\boldsymbol{P}_{a_k}\boldsymbol{H}_{a_k}\boldsymbol{V}_{a_i} = \frac{\mathscr{a}}{\sqrt{N}}\sum_{s=1}^{2}\left(\boldsymbol{w}_{s\,a_k} \otimes \left(\boldsymbol{D}_{s\,a_k}\widetilde{\boldsymbol{h}}_{f_k a_k}\right)\right)\sqrt{\gamma_{a_k}}$$

$$\times \sqrt{\gamma_{a_k}}\left(\boldsymbol{I}_T \otimes \boldsymbol{h}_{a_k}\right)\left(\boldsymbol{v}_{a_i} \otimes \boldsymbol{I}_N\right)$$

$$= \frac{\mathscr{a}}{\sqrt{N}}\sqrt{\gamma_{a_k}}\sum_{s=1}^{2}\left(\boldsymbol{w}_{s\,a_k}\boldsymbol{v}_{a_i}\right) \otimes \boldsymbol{D}_{s\,a_k}\widetilde{\boldsymbol{h}}_{f_k a_k}\boldsymbol{h}_{a_k},$$

where by Def. 1, for all s, $\boldsymbol{w}_{s\,a_k}\boldsymbol{v}_{a_i} = 0$, if $i \neq k$. For $i = k$, the remaining term is eq. (12). Coefficient of $\boldsymbol{u}_{\,f_k}$:

$$\boldsymbol{P}_{a_k}\boldsymbol{H}_{f_k a_k}\boldsymbol{V}_{f_k} = \frac{\mathscr{b}}{\sqrt{M_r}}\sum_{s=1}^{2}\left(\boldsymbol{w}_{s\,a_k} \otimes \left(\boldsymbol{D}_{s\,a_k}\widetilde{\boldsymbol{h}}_{f_k a_k}\right)\right)$$

$$\times \sqrt{\gamma_{f_k a_k}}\left(\boldsymbol{I}_T \otimes \boldsymbol{h}_{f_k a_k}\right)\left(\sum_{i=1}^{T} \xi_{i\,f_k}^{T} \otimes \boldsymbol{r}_i\boldsymbol{q}_i\right)$$

$$= \frac{\mathscr{b}}{\sqrt{M_r}}\sqrt{\gamma_{f_k a_k}}\sum_{s=1}^{2}\sum_{k=1}^{T}\boldsymbol{w}_{s\,a_k}{}^{T}\xi_{i\,f_k}^{T} \otimes \boldsymbol{D}_{s\,a_k}\widetilde{\boldsymbol{h}}_{f_k a_k}\boldsymbol{h}_{f_k a_k}\boldsymbol{r}_i\boldsymbol{q}_i,$$

where for $s = 1$: $\boldsymbol{D}_{s\,a_k}\widetilde{\boldsymbol{h}}_{f_k a_k}\boldsymbol{h}_{f_k a_k}\boldsymbol{r}_i = 0$. Pre-multiplying by $\boldsymbol{D}_{s\,a_k}$ selects a row of $\widetilde{\boldsymbol{h}}_{f_k a_k}$ and post-multiplying by $e_1 = \boldsymbol{r}_i$ for $i = 1, \dots, T-1$, and $e_2 = \boldsymbol{r}_T$ selects a column of $\widetilde{\boldsymbol{h}}_{f_k a_k}$, with the resulting row and column being orthogonal by 4 in Def. 1. For $s = 2$: $\boldsymbol{w}_{s\,a_k}{}^{T}\xi_{i\,f_k}^{T} = 0$ by 2 in Def. 1.■

Example 3. For the example model, $\boldsymbol{P}_{a_1}$ is given by (setting $A = \sqrt{\left(\boldsymbol{h}_{22_{f_1 a_1}}\right)^2 + \left(\boldsymbol{h}_{12_{f_1 a_1}}\right)^2}$ and $B = \sqrt{\left(\boldsymbol{h}_{21_{f_1 a_1}}\right)^2 + \left(\boldsymbol{h}_{11_{f_1 a_1}}\right)^2}$):

$$\boldsymbol{P}_{a_1} = \sum_{s=1}^{2}\left(\boldsymbol{w}_{s\,a_1} \otimes \left(\boldsymbol{D}_{s\,a_1}\widetilde{\boldsymbol{h}}_{f_1 a_1}\right)\right),$$

where $\boldsymbol{w}_{1\,a_1} = \left[-\sqrt{1-c^2} \quad 0 \quad c\right]$, $\boldsymbol{w}_{2\,a_1} = [0 \quad 1 \quad 0]$, $\boldsymbol{\mathcal{D}}_{a_1} = \mathrm{diag}([0 \quad 1]^T)$, $\boldsymbol{\mathcal{D}}_{a_2} = \mathrm{diag}([1 \quad 0]^T)$,

$$\widetilde{\boldsymbol{h}}_{f_1 a_1} = \begin{bmatrix} \dfrac{-\boldsymbol{h}_{22_{f_1 a_1}}}{A} & \dfrac{-\boldsymbol{h}_{12_{f_1 a_1}}}{A} \\ \dfrac{-\boldsymbol{h}_{21_{f_1 a_1}}}{B} & \dfrac{-\boldsymbol{h}_{11_{f_1 a_1}}}{B} \end{bmatrix}.$$

Definition 2. In the neighbouring cells, the rows of the $\mathcal{M} \times M_r T$ projection matrix $\boldsymbol{P}_{f_k} = \boldsymbol{w} \otimes \boldsymbol{W}$ form an orthonormal basis of this subspace, where

1. the $1\times T$ $\boldsymbol{w}$ is a unit vector orthogonal to $\boldsymbol{v}_{a_i}$ for all i,
2. and $\boldsymbol{W}$ is an $\mathcal{M} \times M_r$ all-ones matrix.

Theorem 2. *Multiplying the received signal by projection matrix* $\boldsymbol{P}_{f_k}$*:*

$$\widetilde{\boldsymbol{y}}_{f_k} = \boldsymbol{P}_{f_k}\boldsymbol{y}_{f_k} = \boldsymbol{\mathcal{H}}_{f_k}\boldsymbol{u}_{f_k} + \widetilde{\boldsymbol{z}_{f_k}}, \quad (14)$$

where the $\mathcal{M} \times \mathcal{M}$ *effective channel matrix is given by:*

$$\boldsymbol{\mathcal{H}}_{f_k} = \frac{\mathscr{b}}{\sqrt{M_r}}\boldsymbol{\mathcal{K}}_{f_k}\boldsymbol{\mathcal{D}}_{f_k}, \quad (15)$$

with $\boldsymbol{\mathcal{K}}_{f_k} = \sqrt{\gamma_{f_k}}\boldsymbol{W}\boldsymbol{h}_{f_k}$, $\boldsymbol{\mathcal{D}}_{f_k} = \sum_{i=1}^{T}\boldsymbol{w}\xi_{i\,f_k}^{T}\boldsymbol{r}_i\boldsymbol{q}_i$,

and $\widetilde{\boldsymbol{z}_{f_k.}} = \boldsymbol{P}_{f_k}\boldsymbol{z}_{f_k.}$ *remains white noise with the same variance, since* $\boldsymbol{w}$ *is a unit vector.*

Proof. We show that $\boldsymbol{P}_{f_k}$ removes inter-cell interference at the kth receiver. Substituting eqs. (6) and (8) in eq. (14), the coefficient of $\boldsymbol{u}_{\,a_i}$, for all i, becomes:

$$\boldsymbol{P}_{f_k}\boldsymbol{H}_{Af_k}\boldsymbol{V}_{a_i} = \frac{\mathscr{a}}{\sqrt{N}}(\boldsymbol{w} \otimes \boldsymbol{W})\sqrt{\gamma_{a_k}}\left(\boldsymbol{I}_T \otimes \boldsymbol{h}_{a_k}\right)\left(\boldsymbol{v}_{a_i} \otimes \boldsymbol{I}_N\right)$$

$$= \frac{\mathscr{a}}{\sqrt{N}}\sqrt{\gamma_{a_k}}\sum_{s=1}^{2}\left(\boldsymbol{w}\boldsymbol{v}_{a_i}\right) \otimes \boldsymbol{W}\boldsymbol{h}_{a_k},$$

where by Def. 2, for all i, $\boldsymbol{w}\boldsymbol{v}_{a_i} = 0$. ■

Example 4. For the example model, $\boldsymbol{P}_{f_1}$ is given by:

$$\boldsymbol{P}_{f_1} = \boldsymbol{w} \otimes \boldsymbol{W} = \frac{1}{\sqrt{1+2c^2}}\left[c \quad \sqrt{1-c^2} \quad c\right] \otimes \begin{bmatrix} 1 & 1 & 1 \\ 1 & 1 & 1 \end{bmatrix}.$$

B. Achievable Sum Rate

In the main cell, since there is no CSIT, the rate for each user, for one time slot, is given by:

$$R_{a_k} = \frac{1}{T}\mathbb{E}\left[\mathrm{logdet}\left(\boldsymbol{I}_N + \frac{P_{main\ cell}}{KN^2\sigma_n^2}\right)\right]\boldsymbol{\mathcal{D}}_{a_k}\boldsymbol{\mathcal{K}}_{a_k}\boldsymbol{\mathcal{K}}_{a_k}{}^{*}\boldsymbol{\mathcal{D}}_{a_k}{}^{*}. \quad (16)$$

For any channel realization, in the high SNR limit, the rate is maximized by maximizing: $\det\boldsymbol{\mathcal{D}}_{a_k} = \prod_{s=1}^{2}\left(\boldsymbol{w}_{s\,a_k}\boldsymbol{v}_{\,a_k}{}^{T}\right)$. For the example model, in the high SNR limit, the rate is maximized for $c = -1/\sqrt{3}$.

In a neighbouring cell, since there is no CSIT, the rate for each user, for one time slot, is given by:

$$R_{f_k} = \frac{1}{T}\mathbb{E}\left[\mathrm{logdet}\left(\boldsymbol{I}_{M_r} + \frac{P_{ncell\,F_k}}{\mathcal{M}\sigma_n^2}\right)\right]\boldsymbol{\mathcal{K}}_{f_k}\boldsymbol{\mathcal{D}}_{f_k}\boldsymbol{\mathcal{D}}_{f_k}{}^{*}\boldsymbol{\mathcal{K}}_{f_k}{}^{*}. \quad (17)$$

where by taking $\det\left(\boldsymbol{\mathcal{D}}_{f_k}\boldsymbol{\mathcal{D}}_{f_k}{}^{*}\right)$, the optimal value of d, for the example model, was calculated as $d = \pm 0.5$.

III. Performance Results

Our simulations were based on the example model described and performed in Matlab. The statistical model chosen was i.i.d. Rayleigh and our input symbols were Quadrature Phase Shift Keying (QPSK) modulated. Maximum-Likelihood (ML) detection was performed in the end of the decoding stage. The total transmit power in the mmWave cells was considered as 10W, and therefore a and b, constants determined by power considerations in eqs. (3) and (4), are given $\mathscr{a} = \mathscr{b} = \sqrt{10}$. The path loss exponent was taken as $n = 2$ (Line-of-sight).

Table II. DoF of Blind IA and TDMA

Scheme	Main cell	K Neigh. cells
Blind IA	$\frac{KN}{T}$	$\frac{K\left((K-1)(M_r-1)+1\right)}{T}$
TDMA	$\frac{(T-x)N}{T}$	$\frac{xKM_r}{T}$

A. Degrees of Freedom

Definition 3. As *Degrees of Freedom (DoF*), we define the total number of messages sent over the supersymbol (T).

Table II presents a comparison between Blind IA and TDMA. Based on our simulations, Blind IA outperforms TDMA in the case that we provide more time slots and more antennas.

Theorem 3. *For the Blind IA scheme, the total DoF achieved are given by* $DoF_{Blind\ iA} = K\frac{(N+(K-1)(M_r-1)+1)}{T}$. *For TDMA, setting* $x \in \mathbb{Z}$ *and* $0 < x < T$, *with* x *denoting how many time slots will be given to each cell, the total DoF are given by* $DoF_{TDMA} = K\frac{x(M_r K-N)+NT}{T}$.

B. Bit-Error Rate and Sum Rate

The scheme of Blind IA was compared to the case that only one user is active in the multi-cell mmWave network (ie., to TDMA). The Bit Error Rate (BER) and rate of every user was simulated assuming that only one of them will receive message over $T = 3$ time slots for the TDMA case. Fig. 4 depicts the BER for every user separately, for both Blind IA and TDMA. Overall, looking at the total network performance, Blind IA provides a better performance, especially for SNR values higher than 20dB. Moreover, the scheme of Blind IA always outperforms TDMA for users in the main cell. Regarding BER performance of users in the neighbouring cells, both schemes result in the same BER.

Finally, Fig. 5 shows the comparison, in terms of every user's rate (per time slot), between Blind IA and the TDMA scheme. The rate of the main cell users is better in the Blind IA case, however users in the neighbouring cells achieve the same performance with both schemes. Overall, Blind IA greatly outperforms TDMA, as for example at 30 dB it results in a 500% higher rate than TDMA.

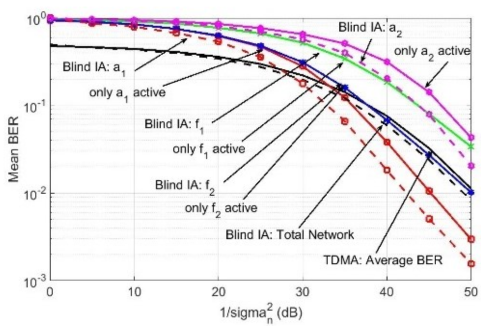

Fig. 4. Blind IA vs. TDMA: BER Performance.

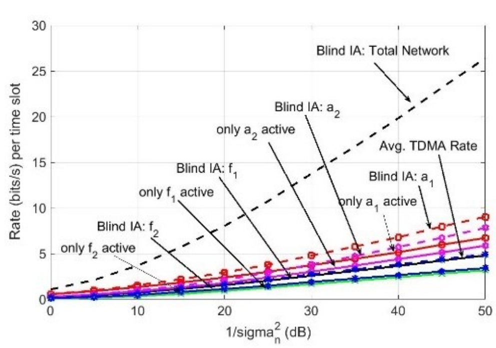

Fig. 5. Blind IA vs. TDMA: Rate Performance

IV. Conclusions

This paper introduces a Blind IA interference management scheme in the multi-cell mmWave network. Although, this paper focuses on the access, as mentioned in Section 1, if users are considered as mmWave APs, the scheme can be employed in fronthaul as well. Overall, the Blind IA scheme provides quite fair scheduling to users in the main cell and achieves higher DoF than TDMA in the case that $M_r = N$. Furthermore, always compared to TDMA, the BER performance of users in the main cell is always better with the scheme of Blind IA, whereas for the neighbouring cell users, the performance is the same. The most important result is the amount by which Blind IA outperforms TDMA regarding the sum rate of the network. This is a significant result, considering the high-rate demand of future networks. Future work will consider a larger number of neighbouring cells interfering with every user in the main cell.

Acknowledgment

The research leading to these results has received funding from the European Commission H2020 programme under grant agreement n671551 (H2020 5G-XHaul project). Also, the authors would like to thank Prof. O. Johnson and Dr. R. Piechocki for their contribution to the initial idea of this paper.

References

[1] Y. Niu, et al, "A survey of millimeter wave communications for 5G Opportunities and Challenges", available online: arxiv.org/abs/1502.07228.

[2] J. Palacios, et al., "Speeding up mmWave beam training through low-complexity hybrid transceivers*", IEEE PIMRC.,* Sept. 2016.

[3] R.W. Heath, et al., "An overview of signal processing tehcniques for millimetre wave MIMO systems", available online: arxiv.org/abs/1512.03007.

[4] J. Wang, "Beam codebook-based beamforming protocol for multi-gbps millimetre-wave WPAN systems*", IEEE J. Sel. Areas Commun*, vol. 27, no. 8, Oct. 2009.

[5] M. Maddah-Ali, A. Motahari, A. Khandani, "Communication over MIMO X channels: Interference alignment, decomposition, and performance analysis", *IEEE Trans. Inf. Theory*, vol. 54, no. 8, Aug. 2008.

[6] S.A. Jafar, S. Shamai, "Degrees of Freedom Region of the MIMO X Channel", *IEEE Trans. Inf. Theory*, vol. 54, no. 1, Jan. 2008.

[7] V.R. Cadambe, S.A. Jafar, "Interference Alignment and Degrees of Freedom of the K-User Interference Channel*", IEEE Trans. Inf. Theory* vol. 54, no. 8, Aug. 2008.

[8] T. Goum, C. Wang, S.A. Jafar, "Aiming Perfectly in the Dark-Blind Interference Alignment Through Staggered Antenna Switching", *IEEE Tran. Signal Process.*, vol. 59, no. 6, pp. 2734-2744, June 2011.

[9] S.A. Jafar, "Blind Interference Alignment", *IEEE J. Sel. Topics Signal Process.*, vol. 6, no. 3, June 2012.

[10] S.A. Jafar, "Elements of Cellular Blind Interference Alignment-Aligned Frequency Reuse, Wireless Index Coding and Interference Diversity", available online: arxiv.org/abs/1203.2384.

[11] V. Kalokidou, O. Johnson, R. Piechocki, "Blind Interference Alignment in General Heterogeneous Networks", *IEEE PIMRC*, Washington D.C., Sept. 2014.

[12] J. Song, et al., "On the Feasibility of Interference Alignment in Ultra-Dense Millimeter-Wave Cellular Networks", *IEEE Asilomar Conference on Signals, Systems and Computers,* pp. 1176-1180, Pacific Grove, Nov. 2016.

[13] C. Wang, et al., "Low Complexity Interference Alignment for mmWave MIMO Channels in Three-Cell Mobile Networks", *IEEE J. Sel. Areas Commun,* vol. 35, no. 7, July 2017.

[14] A. Alkhateeb, et al., "Channel Estimation and Hybrid Precoding for millimeter Wave Cellular Systems", *IEEE J. Sel. Topics Signal Process.*, vol. 8, no. 5, Oct. 2014.